Supplemental Material for Severson *et al.*

The axial element protein HTP-3 promotes cohesin loading and meiotic axis assembly in *C. elegans* to implement the meiotic program of chromosome segregation

Aaron F. Severson, Lorraine Ling, Vanessa van Zuylen and Barbara J. Meyer

Howard Hughes Medical Institute and Department of Molecular and Cell Biology,

University of California, Berkeley, CA USA

Table of Contents

Supplemental Results

REC-8 is required for meiotic crossover recombination

Because sister chromatids separate equationally during anaphase I of *rec-8*(*ok978*) hermaphrodites, meiotic recombination on the X chromosome was assayed as follows: *rec-8*(*ok978*) IV; *dpy-3*(*e27*) *unc-3*(*e151*)/+ + X hermaphrodites were mated with *qIs54* males, and the frequency of Unc non-Dpy and Dpy non-Unc animals was quantified in the triploid male progeny (genotype 3A:2X). In the absence of recombination, these animals would bear a sister chromatid from each X homolog and therefore be of genotype *dpy-3*(*e27*) *unc-3*(*e151*)/+ +. If CO recombination occurs but homologs later separate because of a defect in short arm cohesion, approximately 25% of animals in which recombination occurred in the ~40 cM that separate *dpy-3* and *unc-3* should be Dpy non-Unc or Unc non-Dpy. Because the progeny of *rec-8* mothers are occasionally Unc or Dpy, a parallel control was done using *rec-8*(*ok978*) single mutants. 4.5% (n=223) of males produced by control animals were Unc non-Dpy or Dpy non-Unc, compared to 3.5% (n=257) of males produced by the experimental set of worms. Thus, CO recombination does not occur at appreciable levels during oocyte meiosis of *rec-8* mutant worms.

Supplemental Methods

Validation of ChrII-RFLP data

Data for an entire 96-well PCR plate was discarded if any digests of DNA from control wells containing *n1012* and *n1020* homozygous embryos were incomplete. Data from all embryos collected from a single cross (mutant mother x *him-8*; *mIs10* male) were discarded if all of the embryos from that cross had only one of the two ChrII-RFLPs, because the mother was not trans-heterozygous for the RFLP alleles. Data for a single PCR well were discarded if an uncut band was not detected in the Spe I Xba I double digest, because the embryo analyzed was not outcross.

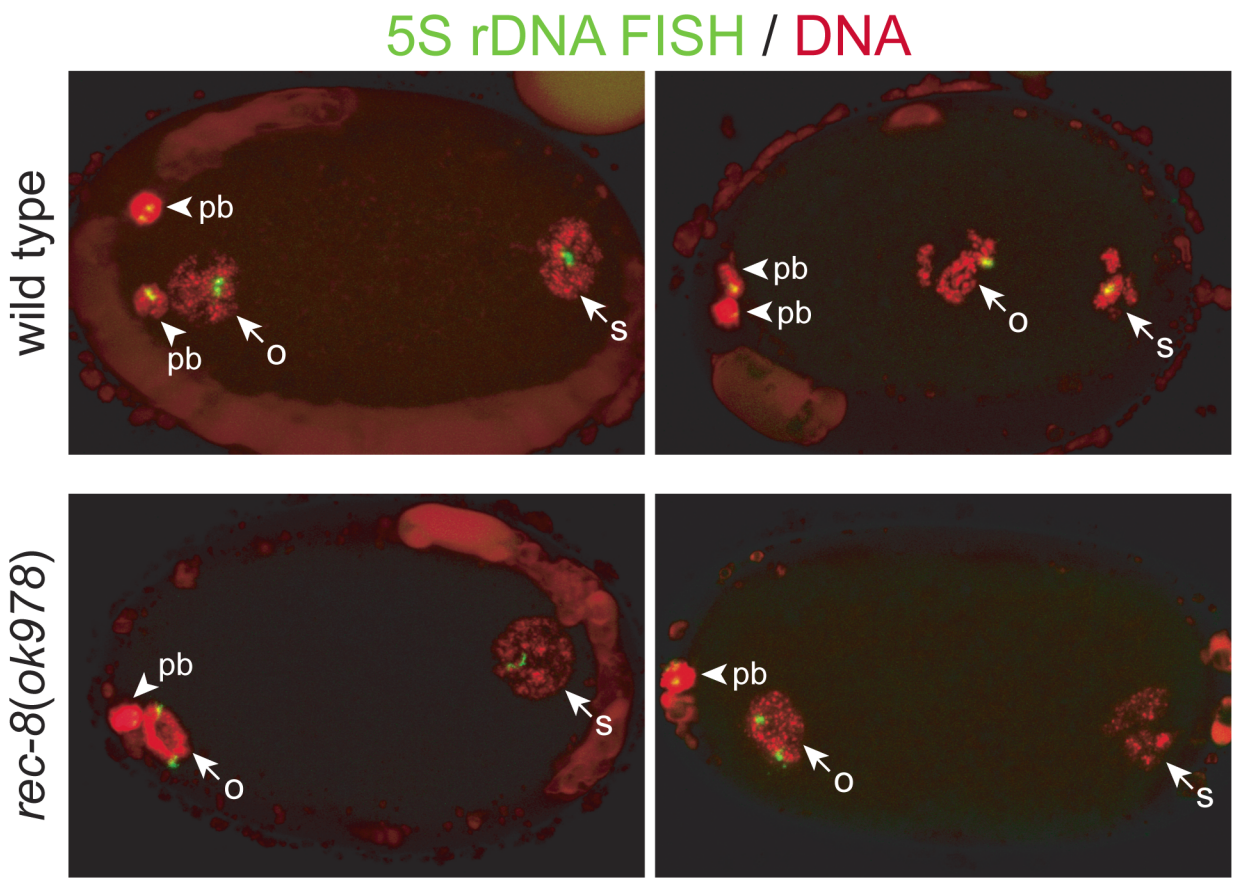

Figure S1. Fluorescence *in situ* hybridization (FISH) demonstrates that zygotes produced by *rec-8(ok978)* mutant mothers inherit two copies of chromosome V during oocyte meiosis. Embryos were labeled with a FISH probe to the 5S rDNA locus (green) and DAPI (red). FISH spots mark the location of chromosome V in the polar bodies (pb), oocyte pronuclei (o) and sperm pronuclei (s). A single FISH spot, corresponding to a single copy of chromosome V, is detected in the haploid oocyte pronucleus of each wild-type embryo. Two FISH spots are detected in the oocyte pronucleus of each *rec-8* zygote, as expected because *rec-8* mutants inherit a sister chromatid from each homolog during oocyte meiosis (Fig. 2C).

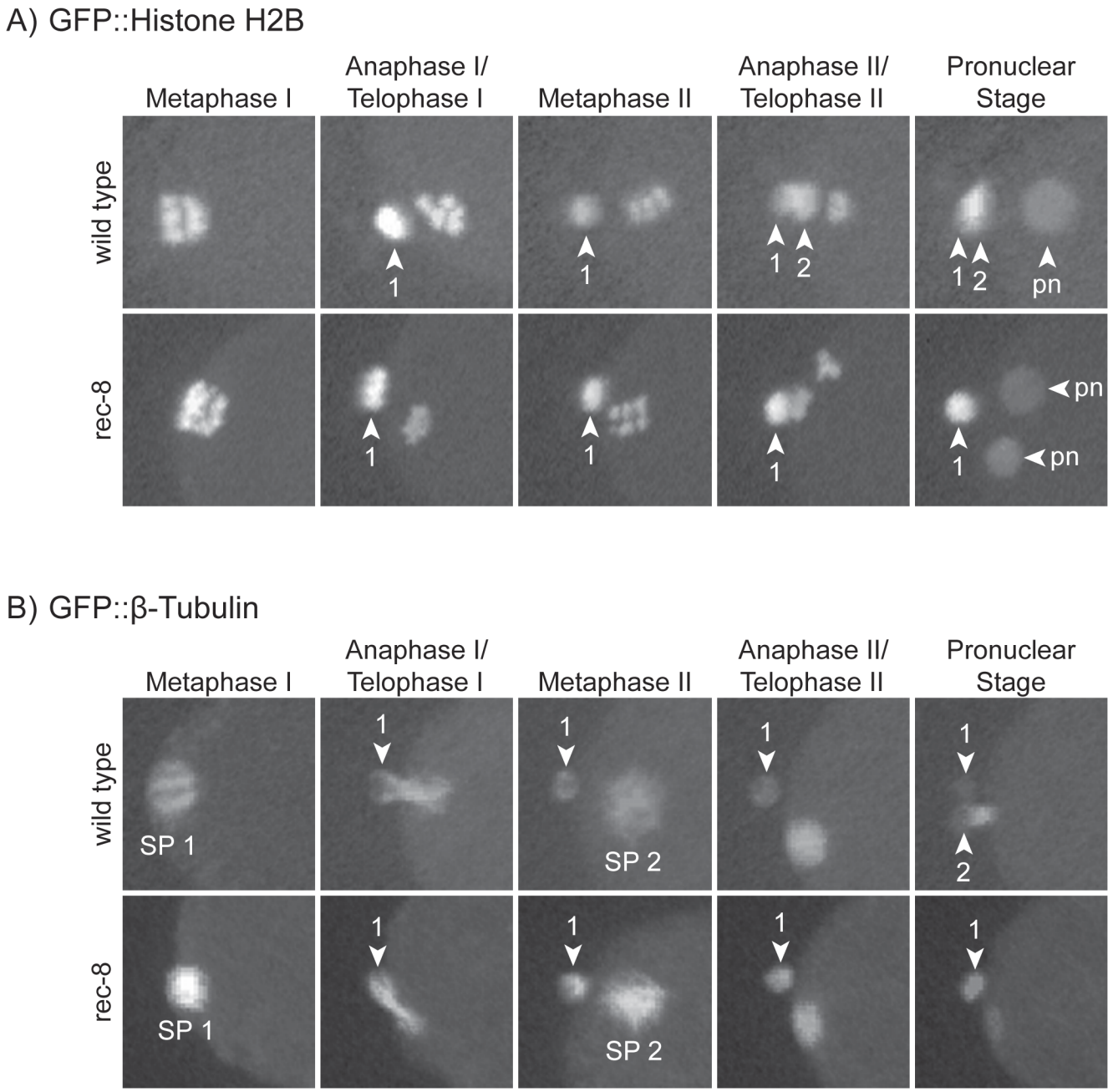

Figure S2. Polar body extrusion fails during meiosis II of *rec-8* mutants.
Two rounds of polar body extrusion can be observed in wild-type zygotes expressing GFP::Histone H2B (A) and GFP::β tubulin (B). (A) Homologous chromosomes separate in anaphase I, and one set of homologs is extruded into the first polar body (1). Sister chromatids separate in anaphase II, and one set of sisters is extruded into the second polar body (2). The second set of sisters decondenses to form the haploid oocyte pronucleus (pn). In contrast, a single polar body is extruded following the equational separation of sister chromatids that occurs in anaphase I of *rec-8(ok978)* mutants. Often, a failed attempt at polar body extrusion in anaphase II results in the formation of multiple pronuclei (pn). (B) Meiotic spindles (SP) assemble during meiosis I (SP 1) and meiosis II (SP 2) of wild-type and *rec-8* mutant zygotes. Thus, two rounds of meiosis occur in *rec-8* mutants, but polar body extrusion fails in meiosis II.

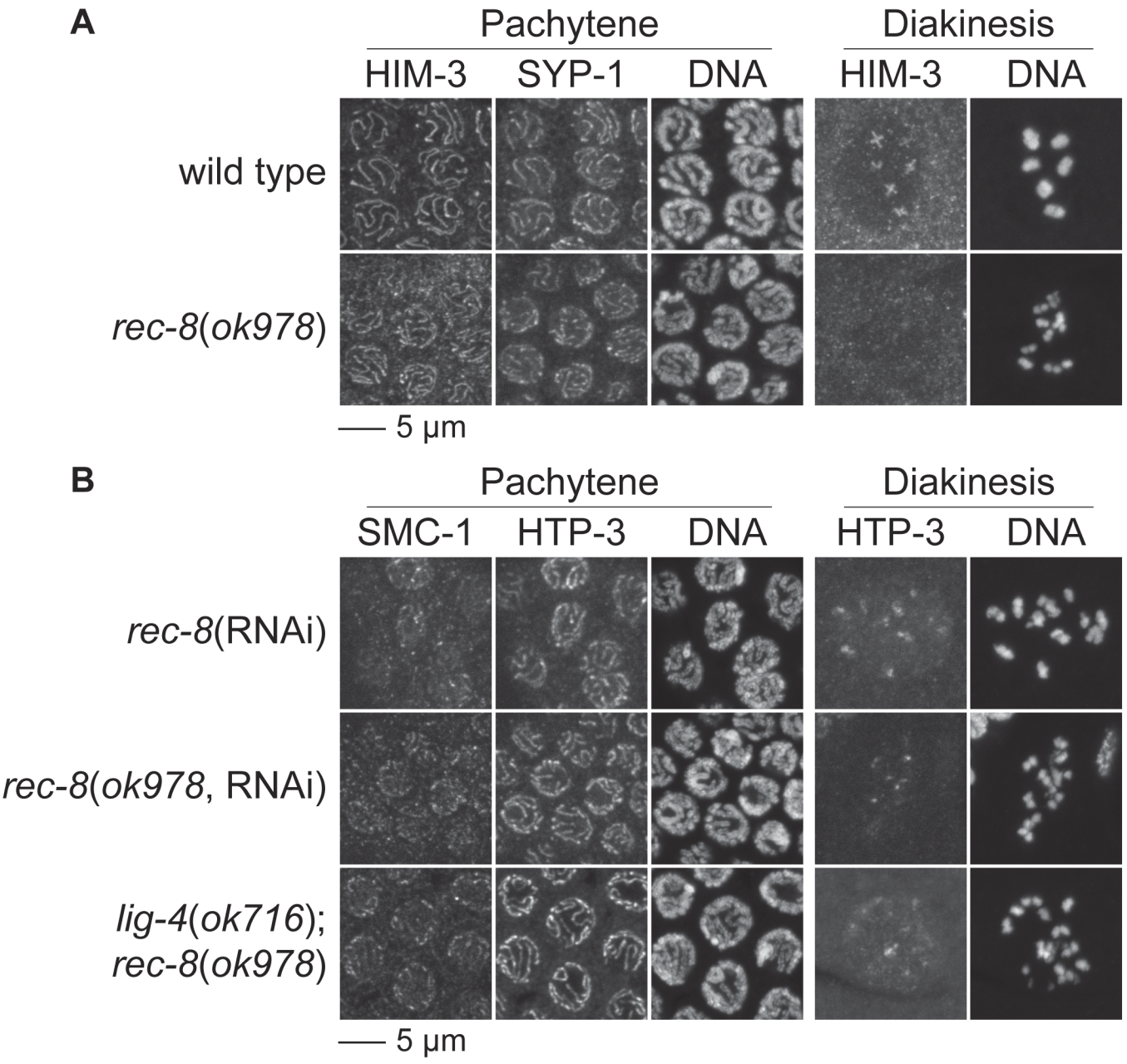
A
Pachytene
Diakinesis
HIM-3
SYP-1
DNA
HIM-3
DNA
wild type
rec-8(ok978)
5 µm
B
Pachytene
Diakinesis
SMC-1
HTP-3
DNA
HTP-3
DNA
rec-8(RNAi)
rec-8(ok978, RNAi)
lig-4(ok716);
rec-8(ok978)
5 µm

Figure S3. *rec-8* mutations fail to block AE assembly and SCC. (A) In wild-type worms, HIM-3 and SYP-1 are present between synapsed pachytene chromosomes. HIM-3 is present in a cruciform on each bivalent in the -1 oocyte. Although HIM-3 levels are reduced in *rec-8*(*ok978*) mutants, long stretches of HIM-3 are clearly visible on pachytene chromosomes. SYP-1 also loads on pachytene chromosomes, but tracks of SYP-1 staining often appear fragmented. (B) Depletion of REC-8 by RNAi results in similar phenotypes to those we observed in *rec-8*(*ok978*) animals. SMC-1 and HTP-3 still associate with meiotic chromosomes in *rec-8*(RNAi) worms; however, SMC-1 levels appear reduced compared to those observed in wild-type worms. 12 univalents are present in diakinesis nuclei. Similar phenotypes are observed when RNAi is used to further reduce REC-8 activity in *rec-8*(*ok978*) mutants, consistent with the prediction that *ok978* is a null or strong loss-of-function allele (Hayashi et al. 2007). The meiotic phenotypes of *rec-8* mutants are not enhanced by a deletion allele of *lig-4*, consistent with the possibility that SCC is required to ensure that a sister chromatid is available for use as a repair template.

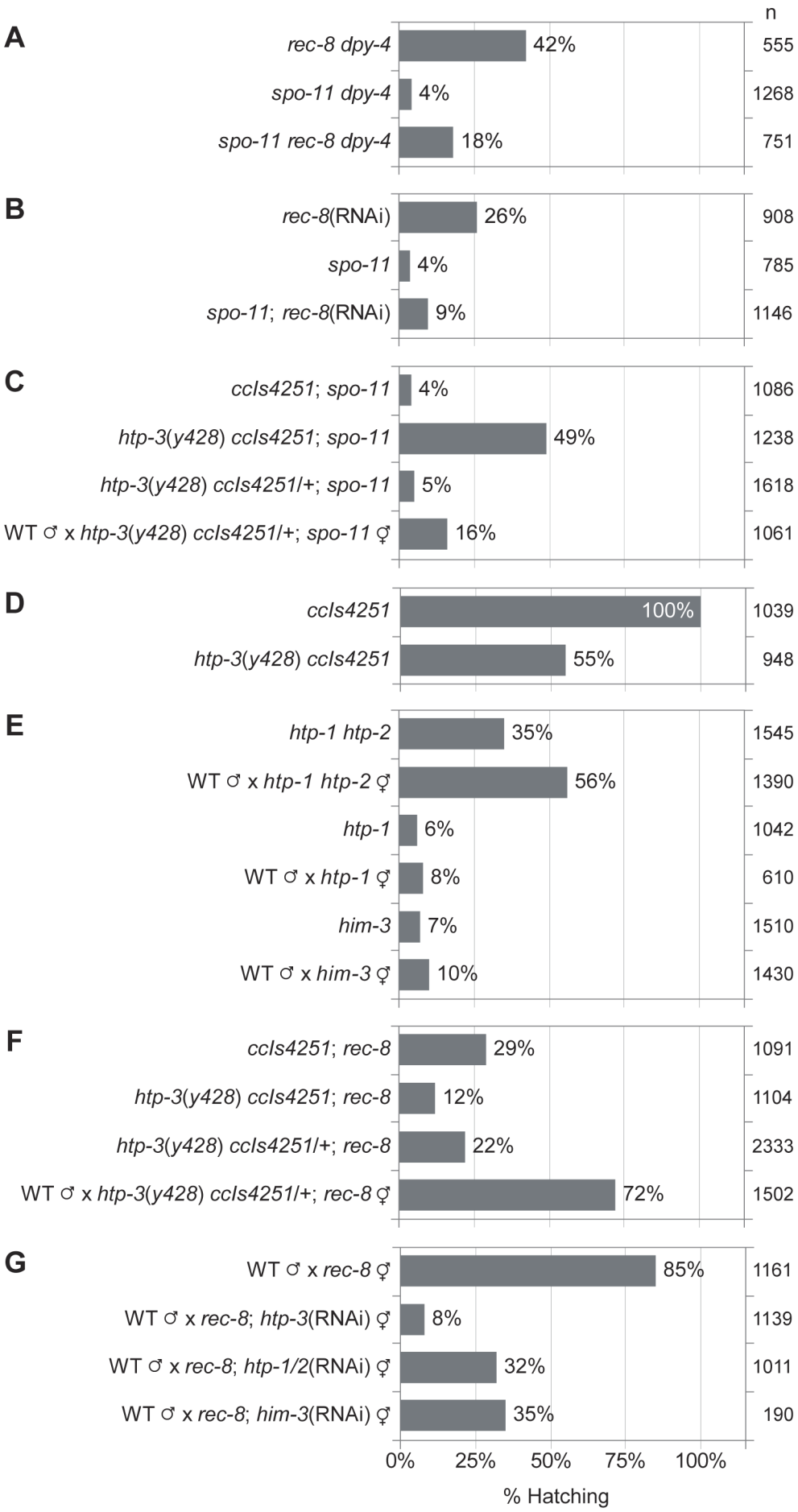
n
A
rec-8 dpy-4
42%
555
spo-11 dpy-4
4%
1268
spo-11 rec-8 dpy-4
18%
751
B
rec-8(RNAi)
26%
908
spo-11
4%
785
spo-11; rec-8(RNAi)
9%
1146
C
ccIs4251; spo-11
4%
1086
htp-3(y428) ccIs4251; spo-11
49%
1238
htp-3(y428) ccIs4251/+; spo-11
5%
1618
WT ♂ x htp-3(y428) ccIs4251/+; spo-11 ♀
16%
1061
D
ccIs4251
100%
1039
htp-3(y428) ccIs4251
55%
948
E
htp-1 htp-2
35%
1545
WT ♂ x htp-1 htp-2 ♀
56%
1390
htp-1
6%
1042
WT ♂ x htp-1 ♀
8%
610
him-3
7%
1510
WT ♂ x him-3 ♀
10%
1430
F
ccIs4251; rec-8
29%
1091
htp-3(y428) ccIs4251; rec-8
12%
1104
htp-3(y428) ccIs4251/+; rec-8
22%
2333
WT ♂ x htp-3(y428) ccIs4251/+; rec-8 ♀
72%
1502
G
WT ♂ x rec-8 ♀
85%
1161
WT ♂ x rec-8; htp-3(RNAi) ♀
8%
1139
WT ♂ x rec-8; htp-1/2(RNAi) ♀
32%
1011
WT ♂ x rec-8; him-3(RNAi) ♀
35%
190
0%
25%
50%
75%
100%
% Hatching

Figure S4. Disrupting REC-8, HTP-3, or HTP-1/2 function reduces the lethality of *spo-11*(*me44*) mutants. (A) Higher embryonic viability is observed in the self progeny of *spo-11*(*me44*) *rec-8*(*ok978*) double mutants than the self progeny of *spo-11*(*me44*) single mutants. (B) Weak suppression of *spo-11*(*me44*) results from RNAi-mediated depletion of REC-8. (C) The *htp-3*(*y428*) allele results in increased viability in the self progeny of *spo-11*(*me44*) worms. This suppression is recessive, as similar levels of embryonic lethality occur in the progeny of *htp-3*(*y428*) *ccIs4251*/+; *spo-11* mutant hermaphrodites as in *spo-11* controls. (D) Most of the self progeny of *htp-3*(*y428*) mothers hatch. Similar levels of hatching are observed in the progeny of *htp-3*(*y428*); *spo-11*(*me44*) animals (C), consistent with the requirement of HTP-3 in DSB formation. (E) Embryonic viability is markedly higher in the broods of *htp-1 htp-2* double mutants than in *htp-1* or *him-3* single mutants, consistent with our data showing that equational sister separation occurs in *htp-1 htp-2* animals, but not in *htp-1* or *him-3* animals. (F) Synergistic lethality occurs in the self progeny of *htp-3*(*y428*); *rec-8*(*ok978*) double mutants. Levels of embryonic lethality in the progeny of *htp-3/+*; *rec-8* animals are similar to those observed in *rec-8* single mutants, consistent with the recessive behavior of the *htp-3*(*y428*) allele. (G) RNAi depletion of HTP-3 in a *rec-8*(*ok978*) mutant worm results in dramatically higher levels of embryonic lethality than does depletion of HTP-1/2 or HIM-3, consistent with the involvement of HTP-3 in the loading of meiotic cohesin.

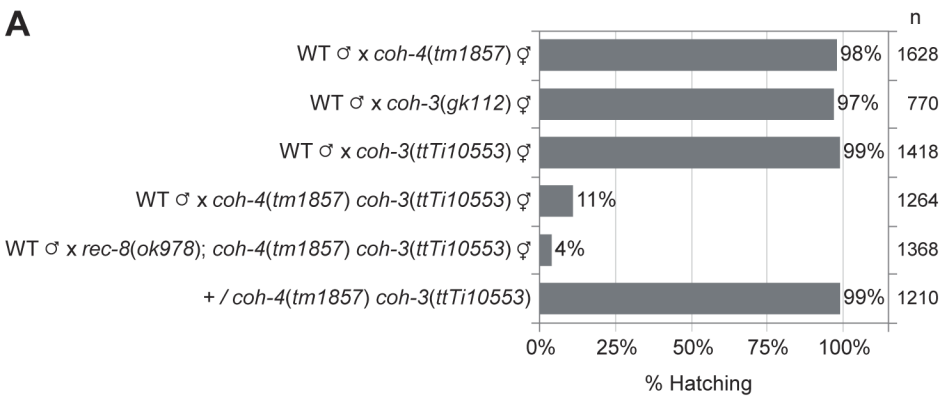
A
n
WT ♂ x coh-4(tm1857) ♀
98%
1628
WT ♂ x coh-3(gk112) ♀
97%
770
WT ♂ x coh-3(ttTi10553) ♀
99%
1418
WT ♂ x coh-4(tm1857) coh-3(ttTi10553) ♀
11%
1264
WT ♂ x rec-8(ok978); coh-4(tm1857) coh-3(ttTi10553) ♀
4%
1368
+ / coh-4(tm1857) coh-3(ttTi10553)
99%
1210
0%
25%
50%
75%
100%
% Hatching

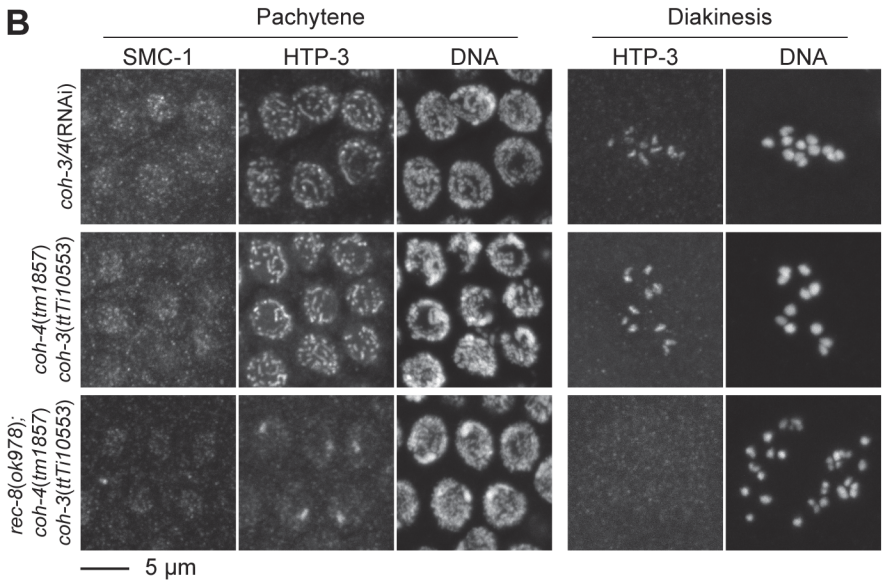
B
Pachytene
Diakinesis
SMC-1
HTP-3
DNA
HTP-3
DNA
coh-3/4(RNAi)
coh-4(tm1857) coh-3(ttTi10553)
rec-8(ok978); coh-4(tm1857) coh-3(ttTi10553)
5 µm

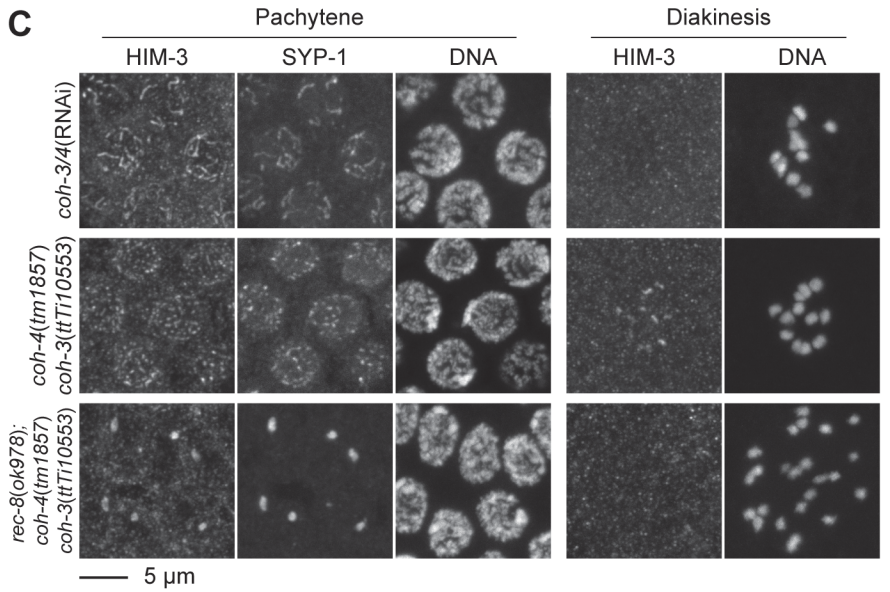
C
Pachytene
Diakinesis
HIM-3
SYP-1
DNA
HIM-3
DNA
coh-3/4(RNAi)
coh-4(tm1857) coh-3(ttTi10553)
rec-8(ok978); coh-4(tm1857) coh-3(ttTi10553)
5 µm

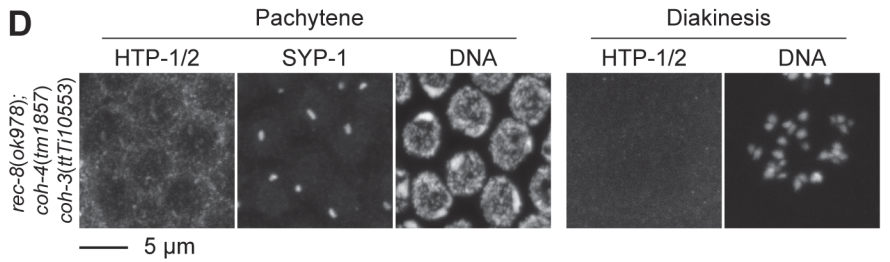
D
Pachytene
Diakinesis
HTP-1/2
SYP-1
DNA
HTP-1/2
DNA
rec-8(ok978); coh-4(tm1857) coh-3(ttTi10553)
5 µm

Figure S5. The redundant kleisin paralogs COH-3 and COH-4 are required for meiotic SCC. (A) Animals mutant for the *coh-4* deletion allele *tm1857*, the *coh-3* deletion allele *gk112*, or the *coh-3* Mos1 transposon insertion allele ttTi10553 produce healthy broods of hatching embryos. In contrast, most embryos produced by *coh-4*(*tm1857*) *coh-3*(*ttTi10553*) double mutants die before hatching, as occurs in *coh-4*(*tm1857*) *coh-3*(*gk112*) double mutants (Fig. 1E). Thus, COH-3 and COH-4 are likely redundant. Almost all progeny of *coh-4*(*tm1857*) *coh-3*(*ttTi10553*) / + heterozygous mothers hatch, suggesting that COH-3 and COH-4 are not essential during mitotic divisions (see also Supplemental Table 1). (B) Depleting COH-3/4 by RNAi does not result in equational sister separation in meiosis I. Instead, homologs appear to segregate randomly. (C) Discontinuous staining of AE proteins is detected on pachytene chromosomes of *coh-4*(*tm1857*) *coh-3*(*ttTi10553*) double mutants and *coh-3/4*(RNAi) animals. In contrast, AE proteins are detected in polycomplexes when COH-3 and COH-4 are disrupted in *rec-8*(*ok978*) mutants.

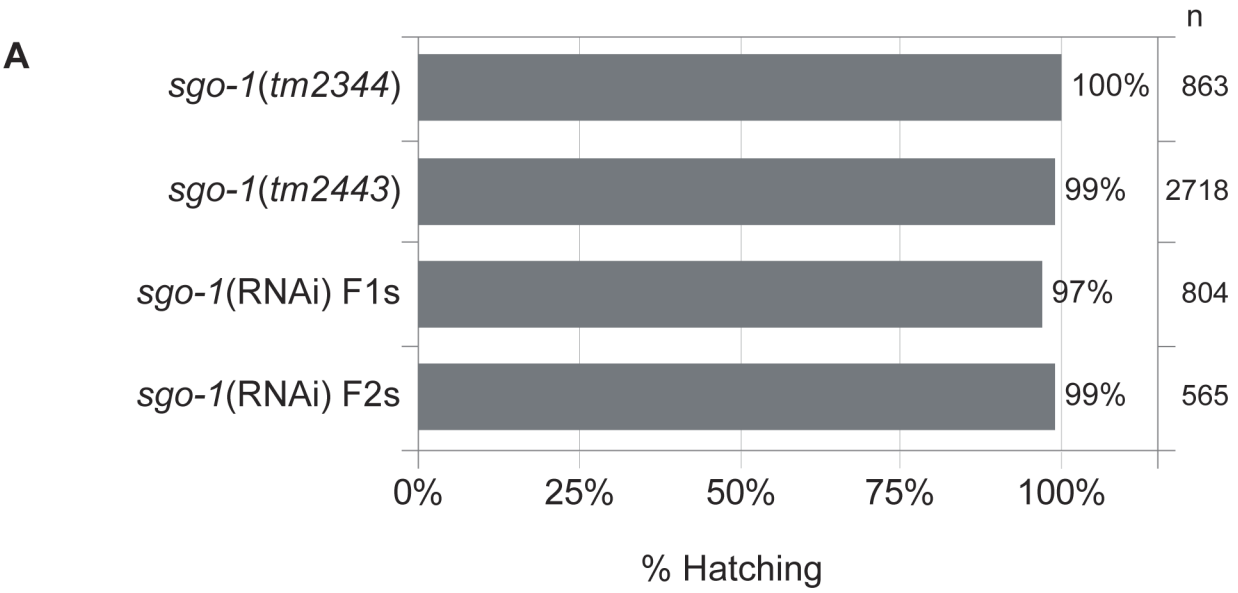
A
n
sgo-1(tm2344)
100%
863
sgo-1(tm2443)
99%
2718
sgo-1(RNAi) F1s
97%
804
sgo-1(RNAi) F2s
99%
565
0%
25%
50%
75%
100%
% Hatching

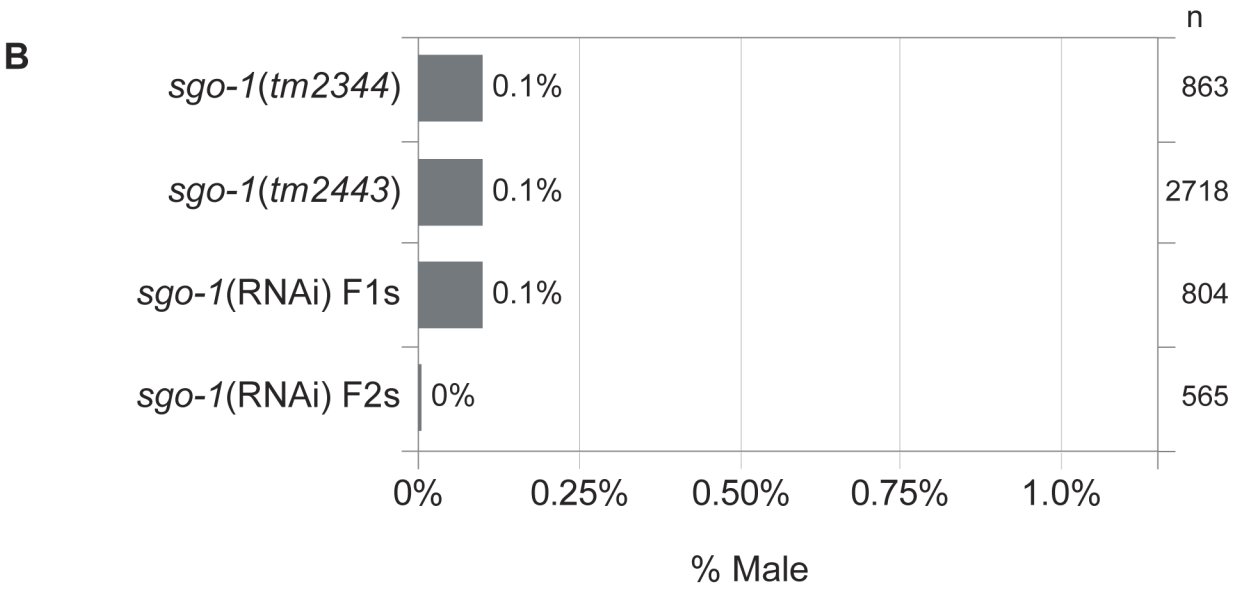
B
n
sgo-1(tm2344)
0.1%
863
sgo-1(tm2443)
0.1%
2718
sgo-1(RNAi) F1s
0.1%
804
sgo-1(RNAi) F2s
0%
565
0%
0.25%
0.50%
0.75%
1.0%
% Male

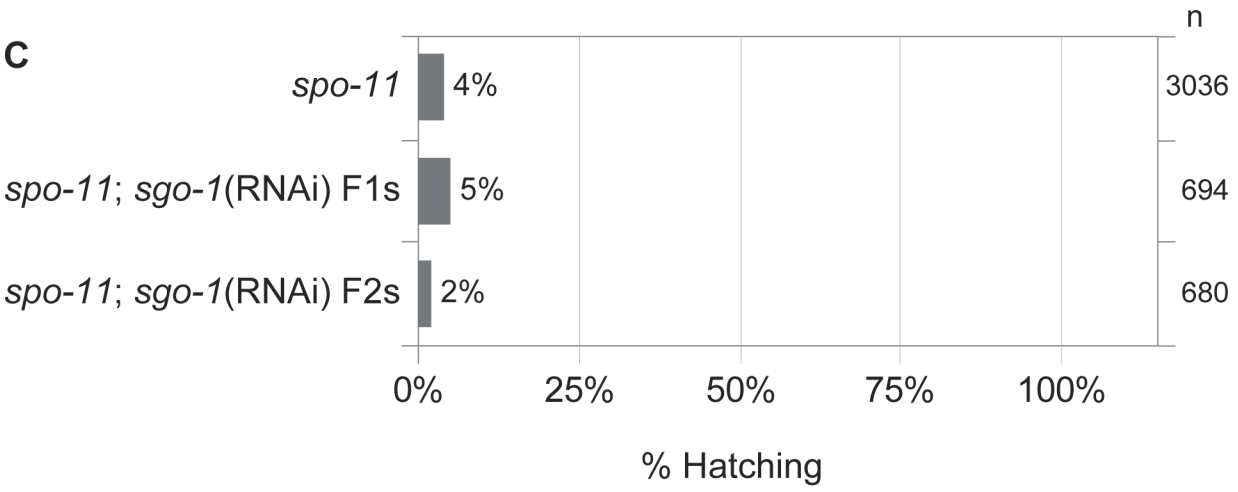
C
n
spo-11
4%
3036
spo-11; sgo-1(RNAi) F1s
5%
694
spo-11; sgo-1(RNAi) F2s
2%
680
0%
25%
50%
75%
100%
% Hatching

Figure S6. The *C. elegans* Mei-S332/Shugoshin ortholog SGO-1 appears dispensable for the accurate segregation of meiotic chromosomes. Embryonic lethality (A) and male production (B) are not observed in animals mutant for either of two *sgo-1* deletion alleles or following *sgo-1*(RNAi). (C) The high levels of embryonic lethality in the broods of *spo-11*(*me44*) mutants is not reduced by RNAi of *sgo-1*.

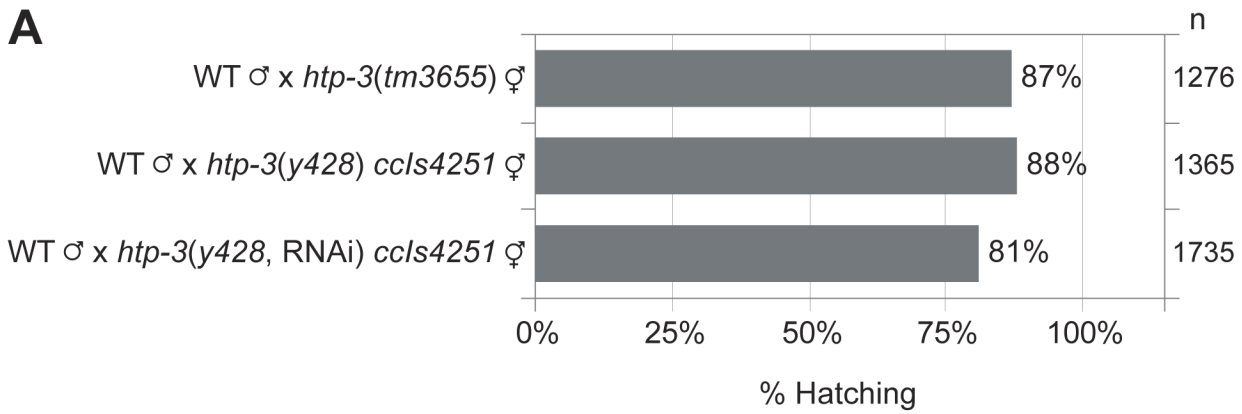
A
n
WT ♂ x htp-3(tm3655) ♀
87%
1276
WT ♂ x htp-3(y428) ccIs4251 ♀
88%
1365
WT ♂ x htp-3(y428, RNAi) ccIs4251 ♀
81%
1735
0%
25%
50%
75%
100%
% Hatching

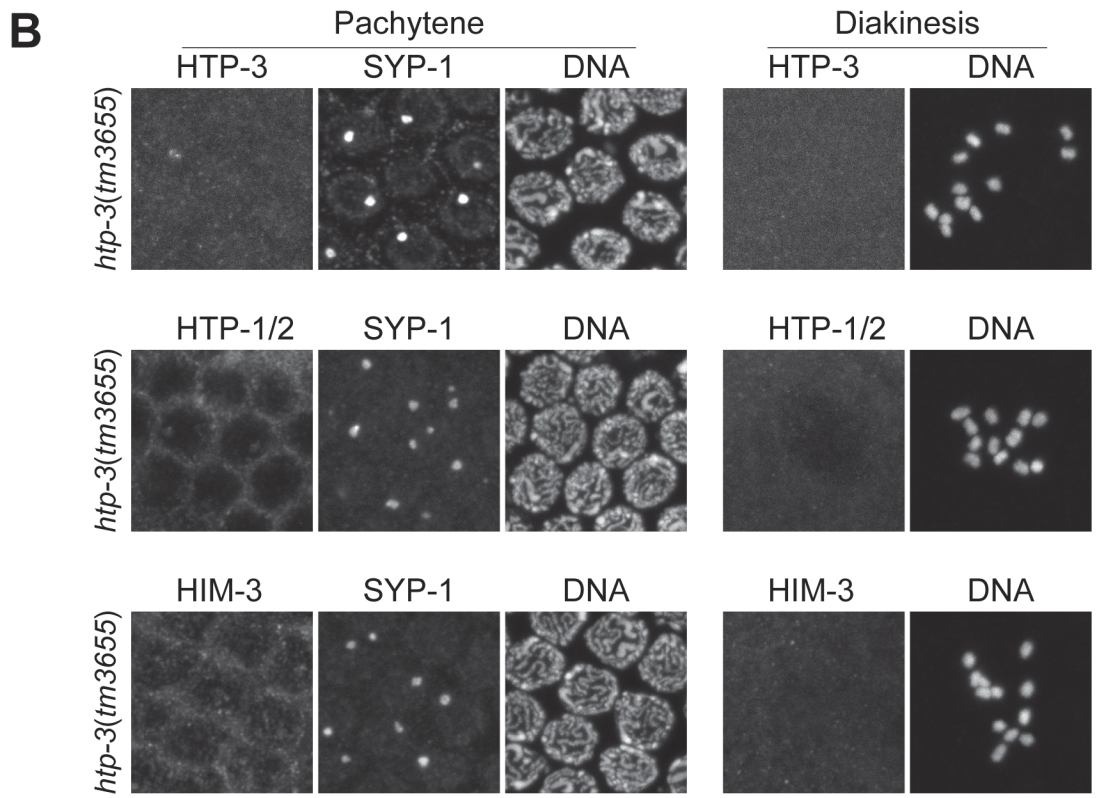
B
Pachytene
Diakinesis
HTP-3
SYP-1
DNA
HTP-3
DNA
htp-3(tm3655)
HTP-1/2
SYP-1
DNA
HTP-1/2
DNA
htp-3(tm3655)
HIM-3
SYP-1
DNA
HIM-3
DNA
htp-3(tm3655)

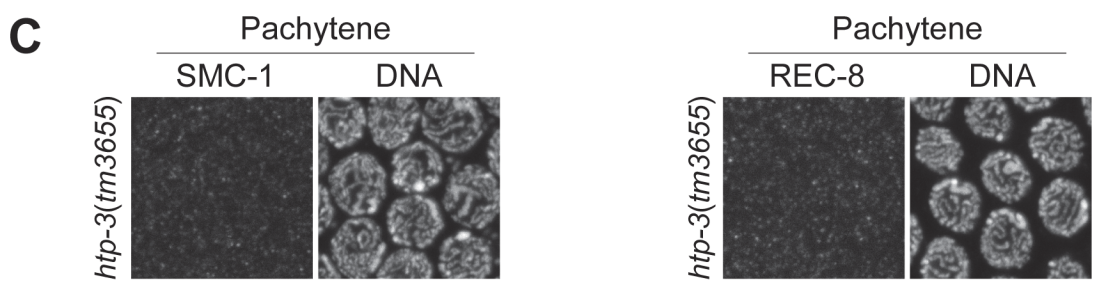
C
Pachytene
SMC-1
DNA
htp-3(tm3655)
Pachytene
REC-8
DNA
htp-3(tm3655)

Figure S7. The *htp-3* deletion allele *tm3655* phenocopies *htp-3*(*y428*). (A) Similar levels of embryonic lethality occur in the broods of *htp-3*(*tm3655*) and *htp-3*(*y428*) mutants. (B) *htp-3(tm3655)* disrupts association of the known AE proteins HTP-3, HTP-1/2, and HIM-3 with the axes of meiotic chromosomes, and the SC central element protein SYP-1 is present in polycomplexes. A similar phenotype occurs in *htp-3*(*y428*) mutants, suggesting that *htp-3*(*y428*) is a null or severe loss-of-function allele (Fig. 8). (C) REC-8 and SMC-1 are undetectable on meiotic chromosomes of *htp-3*(*tm3655*) mutants or *htp-3*(*y428*) mutants (Fig. 9).

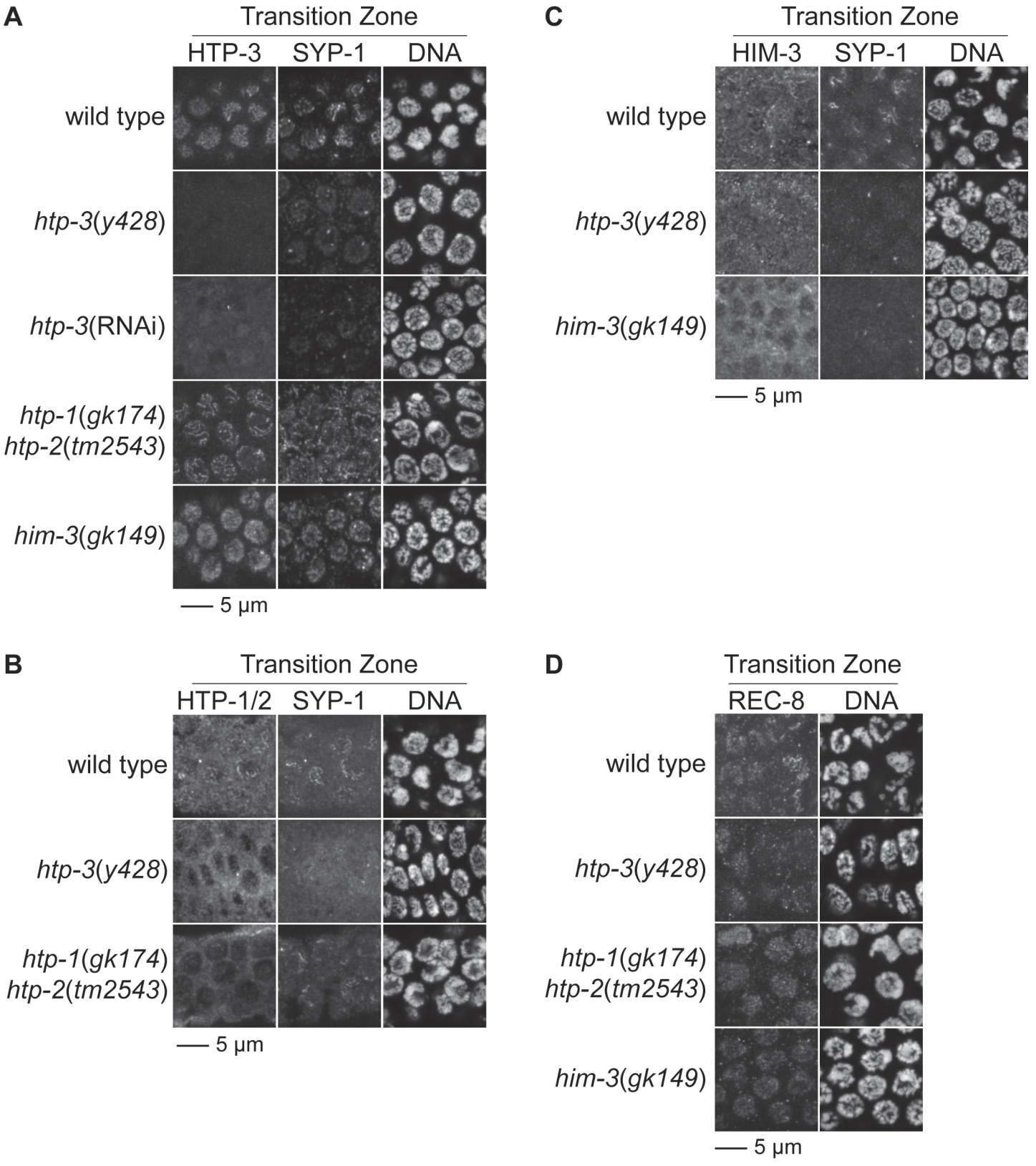
A
Transition Zone
HTP-3
SYP-1
DNA
wild type
htp-3(y428)
htp-3(RNAi)
htp-1(gk174)
htp-2(tm2543)
him-3(gk149)
5 µm
B
Transition Zone
HTP-1/2
SYP-1
DNA
wild type
htp-3(y428)
htp-1(gk174)
htp-2(tm2543)
5 µm
C
Transition Zone
HIM-3
SYP-1
DNA
wild type
htp-3(y428)
him-3(gk149)
5 µm
D
Transition Zone
REC-8
DNA
wild type
htp-3(y428)
htp-1(gk174)
htp-2(tm2543)
him-3(gk149)
5 µm

Figure S8. HTP-3 is required for AE assembly in transition zone nuclei. (A) HTP-3 is present in both premeiotic nuclei and meiotic nuclei, but first associates with axial structures in transition zone nuclei (leptotene and zygotene stages of prophase I). Meiotic loading of HTP-3 does not require HTP-1/2 or HIM-3. SYP-1 is present in polycomplexes in transition zone nuclei of *htp-3*(*y428*) mutants, as in *htp-3*(RNAi) animals (Goodyer et al. 2008). (B,C) HTP-3 is required for the association of HTP-1/2 and HIM-3 with meiotic chromosomes. (D) Like HTP-3, REC-8 is present in premeiotic nuclei but first appears enriched on the axis in transition zone nuclei. REC-8 is detectible in transition zone nuclei of *him-3* and *htp-1 htp-2* mutants; in contrast, REC-8 is present at markedly reduced levels in transition zone nuclei of *htp-3*(*y428*) animals, although it is present in premeiotic nuclei.

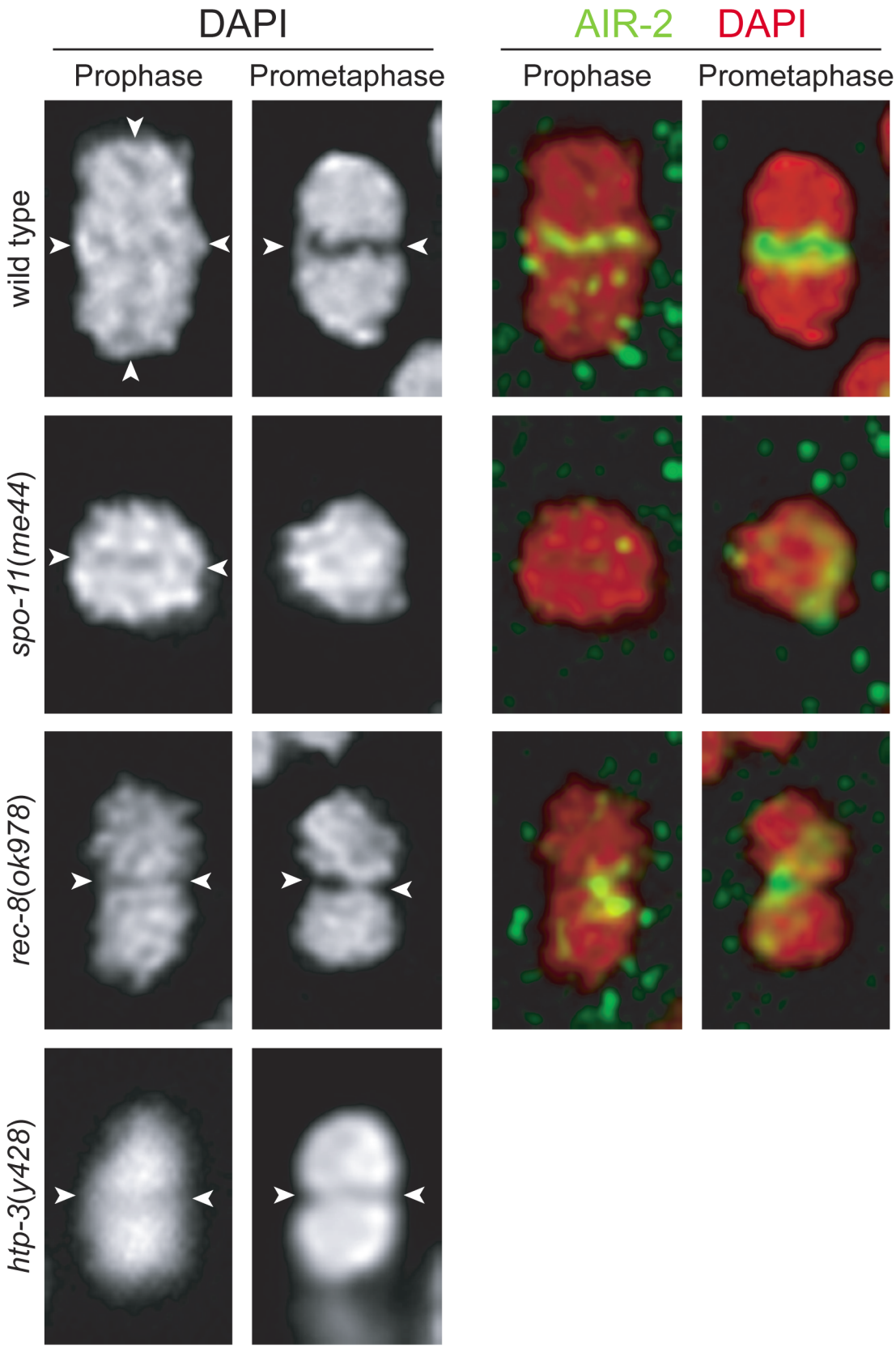
DAPI
AIR-2 DAPI
Prophase
Prometaphase
Prophase
Prometaphase
wild type
spo-11(me44)
rec-8(ok978)
htp-3(y428)

Figure S9. Bivalent structure changes around the time of fertilization and breakdown of the oocyte nuclear envelope. Before fertilization and NEBD, a slight gap separates the four chromatids in DAPI-stained nuclei (arrowheads). In contrast, separation between sisters is not visible after fertilization triggers NEBD and entry into prometaphase, but separation between homologs is obvious (arrowheads). AIR-2 (green) marks the short arm of the wild-type bivalent, where SCC will be released at anaphase I to allow homologs to separate. Before NEBD, a gap is visible between the two sister chromatids in the univalents of *spo-11*(*me44*), *rec-8*(*ok978*), and *htp-3*(*y428*) animals (arrowheads). After NEBD, the sisters are not visible in *spo-11* mutants, and our data indicate that sisters are held together while homologs segregate randomly in anaphase I. In contrast, a visible gap persists between sister chromatids after NEBD in *rec-8* and *htp-3* mutants (arrowheads), sister chromatid co-orientation fails and premature release of SCC in anaphase I causes equational separation of sister chromatids.

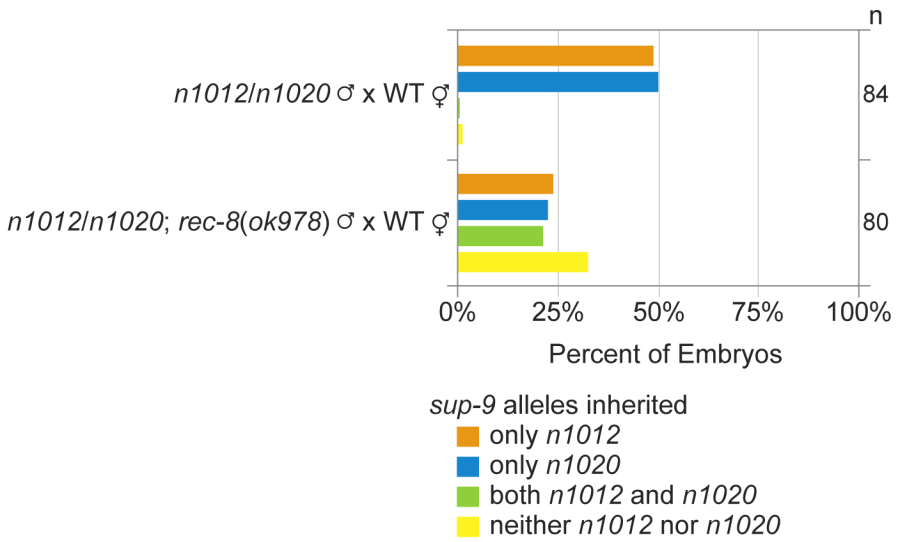

Figure S10. Chromosomes partition randomly during spermatogenesis of *rec-8* mutants, consistent with the possibility that both cytoplasmic divisions occur during spermatogenesis, and sister chromatids separate equationally during meiosis I and randomly during meiosis II.
This pattern of segregation contrasts with that observed during oocyte meiosis of *rec-8* mutants, in which zygotes inherit a sister chromatid from each homolog as a consequence of equational sister separation in meiosis I and defective polar body extrusion in meiosis II. Shown is the assessment of chromosome segregation in wild-type and *rec-8* mutant males using ChrII-RFLP analysis.

Supplemental Table 1. ***Survival to adulthood of strains used in this study***

Genotype [a]	Embryonic Viability [b]	Survival to Adulthood [c]
N2	98%	98%
rec-8(ok978)	85%	54%
spo-11(me44)	10%	7%
ccIs4251[myo-3::GFP]	97%	98%
ccIs4251[myo-3::GFP]; rec-8(ok978)	78%	34%
ccIs4251[myo-3::GFP]; spo-11(me44)	7%	5%
htp-3(y428) ccIs4251[myo-3::GFP]	88%	39%
htp-3(y428) ccIs4251[myo-3::GFP]; rec-8(ok978)	24%	4%
htp-3(y428) ccIs4251[myo-3::GFP]; spo-11(me44)	88%	39%
htp-1(gk174) htp-2(tm2543)	56%	15%
htp-1(gk174)	8%	5%
him-3(gk149)	10%	7%
coh-4(tm1857) coh-3(gk112)	12%	7%
+ /coh-4(tm1857) coh-3(gk112) [d]	100%	99%
rec-8(ok978); coh-4(tm1857) coh-3(gk112)	0.10%	0%

[a] Hermaphrodites of the genotypes listed were mated with *him-8*(*e1489*) IV; *mIs10*[*myo-2::gfp*] males.

[b] Embryonic viability was calculated as: (number of embryos that hatched)/(number of embryos laid)x100.

[c] Survival to adulthood was calculated as: (number of adult worms)/(number of embyros that hatched)x100.

[d] ¼ of embryos laid are expected to be *coh-4(tm1857) coh-3(gk112)* homozygotes. The high survival of these animals suggests that COH-3/4 do not have essential mitotic roles.

Supplemental Table 2. ***Different patterns of meiotic chromosome segregation result in distinct phenotypes***

Chromosome State	Segregation pattern		# of Polar Bodies	Expected frequency of ChrII-RFLPs				Oocyte Ploidy
	Meiosis I	Meiosis II		A and B	Only A	Only B	Neither A or B	
Bivalents [a]	Reductional [c]	Equational [e]	2	0%	50%	50%	0%	Haploid
Univalents [b]	Random [d]	Equational [e]	2	25%	25%	25%	25%	Aneuploid
Univalents [b]	Random [d]	None	1	25%	25%	25%	25%	Aneuploid
Univalents [b]	Equational [e]	Random [f]	2	25%	25%	25%	25%	Aneuploid
Univalents [b]	Equational [e]	None	1	100%	0%	0%	0%	Diploid
Univalents [b]	None	None	0	100%	0%	0%	0%	Tetraploid

[a] Observed in wild-type animals. Homologs are held together by sister chromatid cohesion (SCC) and the crossover.

[b] Observed in mutants that disrupt meiotic crossover recombination. Sister chromatids are held together by SCC, but homologs remain apart.

[c] Homologs separate and move toward opposite spindle poles. Sister chromatids remain held together by SCC.

[d] Homologs partition randomly between the embryo and the polar body. Sister chromatids remain held together by SCC.

[e] Sister chromatids separate and move toward opposite spindle poles.

[f] Sister chromatids partition randomly between the embryo and the polar body.

Supplemental Table 3. ***Strains used in this study***

Strain	Genotype
RB0873	*lig-4(ok716) III*
TY5074	*lig-4(ok716) III; rec-8 (ok978) / nT1 IV; + / nT1 [qIs51] V*
TY4960	*rec-8(ok978) / nT1 IV; + / nT1 [qIs51] V*
TY4342	*spo-11(me44) / nT1 IV; + / nT1 [qIs51] V*
TY4392	*unc-119(ed3op) ruIs32[unc-119(+) pie-1::gfp::his-11] III; rec-8(ok978) / nT1[unc-?(n754) let-?] IV; + / nT1 V*
TY4393	*rec-8(ok978) / nT1[unc-?(n754) let-?] IV; + / nT1 V; ruIs57[unc-119(+) pie-1::gfp::tbb-2] ?*
TY4544	*rec-8(ok978) dpy-4(e1166) / nT1 IV; + / nT1 [qIs51] V*
TY4561	*spo-11(me44) dpy-4(e1166) / nT1 IV; + / nT1 [qIs51] V*
TY4581	*spo-11(me44) rec-8 (ok978) dpy-4(e1166) / nT1 IV; + / nT1 [qIs51] V*
TY4949	*spo-11(me44) rec-8(ok978) / nT1 IV; + / nT1 [qIs51] V*
TY5001	*rec-8(ok978) / nT1 IV; + / nT1 [qIs51] V; dpy-3(e27) unc-3(e151) X*
TY4939	*ccIs4251[myo-3::GFP] I; spo-11(me44) / nT1 [unc-?(n754) let-?(m435)] IV; + / nT1[qIs51] V; lin-2(e1309) X*
TY4980	*htp-3(y428) ccIs4251[myo-3::GFP] / + I; spo-11(me44) / nT1 IV; + / nT1 [qIs51] V*
TY4981	*htp-3(y428) ccIs4251[myo-3::GFP] / + I; rec-8(ok978) / nT1 IV; + / nT1 [qIs51] V*
TY4986	*htp-3(y428) ccIs4251[myo-3::GFP] I / hT2[bli-4(e937) let-?(q782) qIs48] (I;III)*
TY5038	*htp-3(tm3655) I / hT2[bli-4(e937) let-?(q782) qIs48] (I;III)*
TY5115	*coh-4(tm1857) V*
TY4918	*coh-3(gk112) V*
TY5114	*coh-3(ttTi10553) V*
TY5120	*+ / nT1 IV; coh-4(tm1857) coh-3(gk112) V / nT1 [qIs51] V*
TY5119	*+ / nT1 IV; coh-4(tm1857) coh-3(TTtI10553) V / nT1 [qIs51] V*
TY5121	*rec-8(ok978) / nT1 IV; coh-4(tm1857) coh-3(gk112) / nT1 [qIs51] V*
TY5122	*rec-8(ok978) / nT1 IV; coh-4(tm1857) coh-3(ttTi10553) / nT1 [qIs51] V*
TY5130	*htp-3(y428) ccIs4251[myo-3::GFP] I / hT2[bli-4(e937) let-?(q782) qIs48] (I;III); coh-4(tm1857) coh-3(gk112) / nT1[unc-?(n754) let-?] IV; + / nT1 V*
TY5129	*htp-3(y428) ccIs4251[myo-3::GFP] I / hT2[bli-4(e937) let-?(q782) qIs48] (I;III); coh-4(tm1857) coh-3(ttTi10553) / nT1[unc-?(n754) let-?] IV; + / nT1 V*
VC0418	*him-3(gk149) / nT1 IV; + / nT1 [qIs51] V*
TY4973	*htp-1(gk174) / nT1 IV; + / nT1 [qIs51] V*
FM0002	*htp-1(gk174) htp-2(tm2543) / nT1 IV; + / nT1 [qIs51] V*
TY4236	*him-8(e1489) IV; mIs10 V*
FX2344	*sgo-1(tm2344) IV*
TY4878	*sgo-1(tm2443) IV*

Supplemental Table 3. ***Strains used in this study (continued)***

Strain	Genotype
CB0879	*him-1(e879) I*
TY3090	*him-1(h55) / unc-63(e384) I*
JK2735	*qIs54 X*
TY4985	*ccIs4251[myo-3::GFP] I*
TY4851	*sup-9(n1012) II*
TY4852	*sup-9(n1020) II*
TY5131	*sup-9(n1012) II; rec-8(ok978) / nT1 IV; + / nT1 [qIs51] V*
TY4894	*sup-9(n1020) II; rec-8(ok978) / nT1 IV; + / nT1 [qIs51] V*
TY4895	*sup-9(n1012) II; spo-11(me44) / nT1 IV; + / nT1 [qIs51] V*
TY4896	*sup-9(n1020) II; spo-11(me44) / nT1 IV; + / nT1 [qIs51] V*
TY4916	*sup-9(n1012) II; rec-8(ok978) dpy-4(e1166) / nT1 IV; + / nT1 [qIs51] V*
TY4897	*sup-9(n1020) II; rec-8(ok978) dpy-4(e1166) / nT1 IV; + / nT1 [qIs51] V*
TY4898	*sup-9(n1012) II; spo-11(me44) dpy-4(e1166) / nT1 IV; + / nT1 [qIs51] V*
TY4899	*sup-9(n1020) II; spo-11(me44) dpy-4(e1166) / nT1 IV; + / nT1 [qIs51] V*
TY4930	*sup-9(n1012) II; spo-11(me44) rec-8(ok978) dpy-4(e1166) / nT1 IV; + / nT1 [qIs51] V*
TY5132	*sup-9(n1020) II; spo-11(me44) rec-8(ok978) dpy-4(e1166) / nT1 IV; + / nT1 [qIs51] V*
TY4965	*sup-9(n1012) II; htp-1(gk174) / nT1 IV; + / nT1 [qIs51] V*
TY4966	*sup-9(n1020) II; htp-1(gk174) / nT1 IV; + / nT1 [qIs51] V*
TY4999	*sup-9(n1012) II; htp-1(gk174) htp-2(tm2543) / nT1 IV; + / nT1 [qIs51] V*
TY5000	*sup-9(n1020) II; htp-1(gk174) htp-2(tm2543) / nT1 IV; + / nT1 [qIs51] V*
TY4968	*sup-9(n1012) II; him-3(gk149) / nT1 IV; + / nT1 [qIs51] V*
TY4967	*sup-9(n1020) II; him-3(gk149) / nT1 IV; + / nT1 [qIs51] V*
TY5127	*sup-9(n1012) II; coh-4(tm1857) coh-3(gk112) V/nT1[qIs51] (IV;V)*
TY5128	*sup-9(n1020) II; coh-4(tm1857) coh-3(gk112) V/nT1[qIs51] (IV;V)*
TY5125	*sup-9(n1012) II; coh-4(tm1857) coh-3(ttTi10553) V/nT1[qIs51] (IV;V)*
TY5126	*sup-9(n1020) II; coh-4(tm1857) coh-3(ttTi10553) V/nT1[qIs51] (IV;V)*
TY4987	*htp-3(y428) ccIs4251[myo-3::GFP] I / hT2[bli-4(e937) let-?(q782) qIs48] (I;III); sup-9(n1012) II*
TY4988	*htp-3(y428) ccIs4251[myo-3::GFP] I / hT2[bli-4(e937) let-?(q782) qIs48] (I;III); sup-9(n1020) II*
TY4962	*htp-3(y428) ccIs4251[myo-3::GFP]/+ I; sup-9(n1012) II; spo-11(me44) / nT1 IV; + / nT1 [qIs51] V*
TY4963	*htp-3(y428) ccIs4251[myo-3::GFP]/+ I; sup-9(n1020) II; spo-11(me44) / nT1 IV; + / nT1 [qIs51] V*

Supplemental Table 4. ***Oligos used for amplification of dsRNA templates***

Name	Gene	Sequence (T7 in bold)
AFS75 [a]	*rec-8*	**TAATACGACTCACTATAGG**GGTTGTCTCTGCGGAAGT
AFS76 [a]	*rec-8*	**TAATACGACTCACTATAGG**GCTCAGGTAAGGCTCAACA
AFS268	*htp-3*	**TAATACGACTCACTATAGG**AAGTCCCATCTACGGTCGTG
AFS269	*htp-3*	**TAATACGACTCACTATAGG**CTTTGGAGGGTTTGGTTTGA
AFS279	*htp-1*	**TAATACGACTCACTATAGG**CGTCTGGATAGGCGACATTT
AFS280	*htp-1*	**TAATACGACTCACTATAGG**CATCTACGACGAATCGCTCA
AFS283	*him-3*	**TAATACGACTCACTATAGG**TCCCGTTGATCTAGAGATTGAAA
AFS284	*him-3*	**TAATACGACTCACTATAGG**ACAAGAGAAGACAAAAGCACGAC
AFS191	*him-1*	GCG**TAATACGACTCACTATAGG**GAAGGCAGAGAACAACTCGACTCAG
AFS192	*him-1*	CGC**TAATACGACTCACTATAGG**GATCAGCAGAACCTCCGGACATA
AFS193 [b,c]	*coh-3* 5'	**TAATACGACTCACTATAGG**ATTCGTGCTCGAGAGATCGT
AFS194 [b,c]	*coh-3* 5'	**TAATACGACTCACTATAGG**CGGTTTGGAGTTCCAGTTGT
AFS308 [b,d]	*coh-3* 3'	**TAATACGACTCACTATAGG**TGGTCAAATACAAGTTCTGA
AFS309 [b,d]	*coh-3* 3'	**TAATACGACTCACTATAGG**AGAAATCAGCCATTGCCAGA
AFS79	*sgo-1*	**TAATACGACTCACTATAGG**AGCTTGTCGTCAGTCTCGGT
AFS80	*sgo-1*	**TAATACGACTCACTATAGG**TGCAGGAGTTGATGATGGAG

[a] dsRNA corresponding to Exons 1-4 was used for depletion of REC-8 because this region is not affected by the *rec-8*(*ok978*) deletion. Similar results were obtained using the primers and depletion regime described in Colaiácovo (2003).

[b] dsRNA corresponding to nonoverlapping 5' and 3' regions of the *coh-3* ORF with no significant homology gave similar phenotypes in RNAi experiments, indicating that the phenotypes observed did not result from off target depletion of another cohesin subunit.

[c] The 1674 bp amplicon corresponds to 1263 bp of cDNA, which is 88% identical to the paralogous region of the Y45G5AM.8 cDNA.

[d] The 381 bp amplicon corresponds to 283 bp of cDNA, which is 89% identical to the paralogous region of the Y45G5AM.8 cDNA.